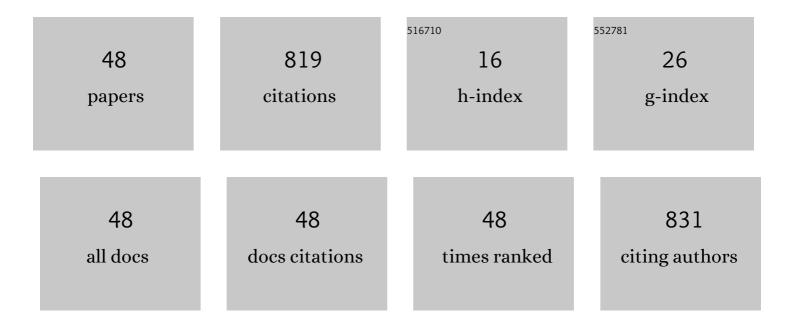
Mingkai Li

List of Publications by Year in descending order

Source: https://exaly.com/author-pdf/4328709/publications.pdf Version: 2024-02-01



MINCKALL

#	Article	IF	CITATIONS
1	Multi-component ZnO alloys: Bandgap engineering, hetero-structures, and optoelectronic devices. Materials Science and Engineering Reports, 2022, 147, 100661.	31.8	58
2	The elastic, electron, phonon, and vibrational properties of monolayer XO2 (XÂ=ÂCr, Mo, W) from first principles calculations. Materials Today Communications, 2022, 30, 103183.	1.9	6
3	High-performance self-driven ultraviolet photodetector based on SnO2 p-n homojunction. Optical Materials, 2022, 129, 112571.	3.6	6
4	Monolayer SnX (X = O, S, Se): Two-Dimensional Materials with Low Lattice Thermal Conductivities and High Thermoelectric Figures of Merit. ACS Applied Energy Materials, 2022, 5, 7802-7812.	5.1	20
5	XTIO (XÂ=ÂK, Rb, Cs): Novel 2D semiconductors with high electron mobilities, ultra-low lattice thermal conductivities and high thermoelectric figures of merit at room temperature. Applied Surface Science, 2022, 599, 153924.	6.1	20
6	Achieving p-type conductivity in wide-bandgap SnO2 by a two-step process. Applied Physics Letters, 2021, 118, .	3.3	12
7	Enhancing visible-light transmittance while reducing phase transition temperature of VO2 by Hf–W co-doping. Applied Physics Letters, 2021, 118, .	3.3	21
8	Conjugated Ditertiary Ammonium Templated (100)-Oriented 2D Perovskite with Efficient Broad-Band Emission. Chemistry of Materials, 2021, 33, 4456-4464.	6.7	23
9	Nb-doped ZrxSn1â^'xO2: Experimental and first-principles study. Journal of Applied Physics, 2021, 130, .	2.5	2
10	Intermolecular Hydrogen-Bonding Correlated Structure Distortion and Broadband White-Light Emission in 5-Ammonium Valeric Acid Templated Lead Chloride Perovskites. Crystal Growth and Design, 2021, 21, 5731-5739.	3.0	13
11	Highâ€Performance Selfâ€Powered Ultraviolet Photodetector based on Coupled Ferroelectric Depolarization Field and Heterojunction Builtâ€In Potential. Advanced Electronic Materials, 2021, 7, 2100717.	5.1	26
12	Antisolventâ€assisted Crystallization of Centimeterâ€sized Leadâ€free Bismuth Bromide Hybrid Perovskite Single Crystals with Xâ€ray Sensitive Merits. Chemistry - an Asian Journal, 2021, 16, 4137-4144.	3.3	10
13	The S-content-dependent lattice structure evolution and bandgap modulation in quaternary MgZnOS alloy films. Journal Physics D: Applied Physics, 2021, 54, 065104.	2.8	1
14	Highly Sensitive and Tunable Self-Powered UV Photodetectors Driven Jointly by p-n Junction and Ferroelectric Polarization. ACS Applied Materials & Interfaces, 2020, 12, 53957-53965.	8.0	65
15	Two-dimensional SnO ultrathin epitaxial films: Pulsed laser deposition growth and quantum confinement effects. Physica B: Condensed Matter, 2020, 599, 412467.	2.7	4
16	RuVO2 alloy epitaxial films: Lowered insulator–metal transition temperature and retained modulation capacity. Applied Physics Letters, 2020, 116, 192103.	3.3	8
17	Size effect on excess resistivity induced by hydrogen in ultra-thin vanadium systems. Physical Chemistry Chemical Physics, 2020, 22, 11609-11613.	2.8	1
18	High performance solar-blind UV detector based on Hf0.38Sn0.62O2 epitaxial film. Applied Physics Letters, 2020, 116, .	3.3	7

Μινςκαι Li

#	Article	IF	CITATIONS
19	The band alignment of nonpolar m-plane ZnO1â^'xSx/Mg0.4Zn0.6O heterojunctions. AIP Advances, 2020, 10, 015314.	1.3	3
20	Effects of oxygen pressure on PLD-grown Be and Cd co-substituted ZnO alloy films for ultraviolet photodetectors. Journal of Alloys and Compounds, 2020, 833, 155032.	5.5	19
21	Electronic structure and dynamic properties of two-dimensional W Mo1â^'S2 ternary alloys from first-principles calculations. Computational Materials Science, 2020, 182, 109797.	3.0	11
22	Photovoltaic effect in <i>m</i> -plane orientated ZnOS epitaxial thin films. Applied Physics Letters, 2019, 115, .	3.3	8
23	Influence of growth temperature on the characteristics of β-Ga2O3 epitaxial films and related solar-blind photodetectors. Applied Surface Science, 2019, 489, 101-109.	6.1	73
24	Pulsed laser deposition and characteristics of epitaxial non-polar m-plane ZnO1-xSx alloy films. Journal of Alloys and Compounds, 2019, 773, 443-448.	5.5	10
25	From stannous oxide to stannic oxide epitaxial films grown by pulsed laser deposition with a metal tin target. Applied Surface Science, 2019, 466, 765-771.	6.1	8
26	Theoretical investigation of the structural, electronic, and thermodynamic properties of CdS1- <i>x</i> Se <i>x</i> alloys. Journal of Applied Physics, 2018, 123, .	2.5	10
27	Electronic-structure and thermodynamic properties of ZnS1â^'Se ternary alloys from the first-principles calculations. Computational Materials Science, 2018, 149, 386-396.	3.0	12
28	Pulsed laser deposited Be x Zn 1-x O 1-y S y quaternary alloy films: structure, composition, and band gap bowing. Applied Surface Science, 2018, 433, 674-679.	6.1	10
29	Conducting Polymer Paper-Derived Mesoporous 3D N-doped Carbon Current Collectors for Na and Li Metal Anodes: A Combined Experimental and Theoretical Study. Journal of Physical Chemistry C, 2018, 122, 23352-23363.	3.1	27
30	Accounting for the thermo-stability of PdHx (xÂ=Â1–3) by density functional theory. International Journal of Hydrogen Energy, 2018, 43, 18372-18381.	7.1	12
31	Greatly enhanced photocurrent in inorganic perovskite [KNbO ₃] _{0.9} [BaNi _{0.5} Nb _{0.5} O _{3â€if}] _{0.1ferroelectric thinâ€film solar cell. Journal of the American Ceramic Society, 2018, 101, 4892-4898.}	uta 8	29
32	Inter-Conversion between Different Compounds of Ternary Cs-Pb-Br System. Materials, 2018, 11, 717.	2.9	29
33	Theoretical investigation on thermodynamic properties of ZnO1â^'xTexalloys. Materials Research Express, 2017, 4, 055901.	1.6	5
34	First-principles calculations of the phase equilibrium of BexZn1â^'xO alloys. Journal of Applied Physics, 2017, 121, 205101.	2.5	8
35	First-principles calculations of the thermodynamics of wurtzite and zincblende ZnO 1-x S x alloys. Physica B: Condensed Matter, 2017, 520, 1-6.	2.7	7
36	Magnetic order and phase diagram of magnetic alloy system: Mg <i>_x</i> Ni _{1–<i>x</i>} O alloy. Physica Status Solidi (B): Basic Research, 2017, 254, 1700085.	1.5	4

Mingkai Li

#	Article	IF	CITATIONS
37	Synthesis of all-inorganic CsPb ₂ Br ₅ perovskite and determination of its luminescence mechanism. RSC Advances, 2017, 7, 54002-54007.	3.6	49
38	SnO2 epitaxial films with varying thickness on c-sapphire: Structure evolution and optical band gap modulation. Applied Surface Science, 2017, 423, 611-618.	6.1	42
39	The S concentration dependence of lattice parameters and optical band gap of a-plane ZnOS grown epitaxially on r-plane sapphire. Journal of Alloys and Compounds, 2015, 630, 106-109.	5.5	14
40	Single-phase quaternary MgxZn1â^'xO1â^'ySy alloy thin films grown by pulsed laser deposition. Journal of Applied Physics, 2015, 117, 065301.	2.5	8
41	Structural properties and enhanced bandgap tunability of quaternary CdZnOS epitaxial films grown by pulsed laser deposition. Journal of Alloys and Compounds, 2015, 650, 748-752.	5.5	11
42	First-principles study of divalent IIA and transition IIB metals doping into Cu2O. Journal Wuhan University of Technology, Materials Science Edition, 2015, 30, 458-462.	1.0	8
43	Annealing and characterisation of CuInS2 thin films prepared on sapphire substrates by pulsed laser deposition. Materials Research Innovations, 2014, 18, S4-22-S4-25.	2.3	Ο
44	Optical properties of the nonpolar a-plane MgZnO films grown on a-GaN/r-sapphire templates by pulsed laser deposition. Optical Materials Express, 2014, 4, 2346.	3.0	7
45	Annealing effects on CuInS2 thin films grown on glass substrates by using pulsed laser deposition. Journal of the Korean Physical Society, 2014, 64, 410-414.	0.7	6
46	Structural and optical properties of single-phase ZnO1â^'S alloy films epitaxially grown by pulsed laser deposition. Journal of Alloys and Compounds, 2014, 587, 369-373.	5.5	23
47	Tuning the composition and optical band gap of pulsed laser deposited ZnO1â^'S alloy films by controlling the substrate temperature. Journal of Alloys and Compounds, 2014, 617, 413-417.	5.5	15
48	Solubility limits and phase structures in epitaxial ZnOS alloy films grown by pulsed laser deposition. Journal of Alloys and Compounds, 2012, 534, 81-85.	5.5	48